Acta Pharmacologica Sinica

ARTICLE

PINK1 overexpression prevents forskolin-induced tau hyperphosphorylation and oxidative stress in a rat model of Alzheimer's disease

Xiao-juan Wang[1], Lin Qi[1], Ya-fang Cheng[1], Xue-fei Ji[1], Tian-yan Chi[1], Peng Liu[1] and Li-bo Zou[1]

PTEN-induced putative kinase 1 (PINK1)/parkin pathway mediates mitophagy, which is a specialized form of autophagy. Evidence shows that PINK1 can exert protective effects against stress-induced neuronal cell death. In the present study we investigated the effects of PINK1 overexpression on tau hyperphosphorylation, mitochondrial dysfunction and oxidative stress in a specific rat model of tau hyperphosphorylation. We showed that intracerebroventricular (ICV) microinjection of forskolin (FSK, 80 μmol) induced tau hyperphosphorylation in the rat brain and resulted in significant spatial working memory impairments in Y-maze test, accompanied by synaptic dysfunction (reduced expression of synaptic proteins synaptophysin and postsynaptic density protein 95), and neuronal loss in the hippocampus. Adeno-associated virus (AAV)-mediated overexpression of PINK1 prevented ICV-FSK-induced cognition defect and pathological alterations in the hippocampus, whereas PINK1-knockout significantly exacerbated ICV-FSK-induced deteriorated effects. Furthermore, we revealed that AAV-PINK1-mediated overexpression of PINK1 alleviated ICV-FSK-induced tau hyperphosphorylation by restoring the activity of PI3K/Akt/GSK3β signaling. PINK1 overexpression reversed the abnormal changes in mitochondrial dynamics, defective mitophagy, and decreased ATP levels in the hippocampus. Moreover, PINK1 overexpression activated Nrf2 signaling, thereby increasing the expression of antioxidant proteins and reducing oxidative damage. These results suggest that PINK1 deficiency exacerbates FSK-induced tau pathology, synaptic damage, mitochondrial dysfunction, and antioxidant system defects, which were reversed by PINK1 overexpression. Our data support a critical role of PINK1-mediated mitophagy in controlling mitochondrial quality, tau hyperphosphorylation, and oxidative stress in a rat model of Alzheimer's disease.

Keywords: PINK1; Forskolin; Tau hyperphosphorylation; PI3K/Akt/GSK3β signaling; mitophagy; Nrf2 signaling; oxidative stress; Alzheimer's disease

Acta Pharmacologica Sinica (2022) 43:1916–1927; https://doi.org/10.1038/s41401-021-00810-5

INTRODUCTION

Alzheimer's disease (AD) is a chronic neurodegenerative disease and the most common cause of dementia. The main symptoms are memory loss and cognitive dysfunction [1]. Neurogenesis in nerve cells containing hyperphosphorylated tau protein aggregates, which are known as neurofibrillary tangles (NFTs), is a histopathological marker of many neurodegenerative diseases, including AD, and these conditions are collectively called tauopathies [2]. Mitochondria are the energy producers of eukaryotic cells. Mitochondrial dysfunction leads to reduced energy production and the release of reactive oxygen species (ROS), resulting in neuronal damage [3]. Mitochondrial abnormalities, including morphological abnormalities, have been found in patients with early-stage AD and in experimental AD tauopathy models [4, 5]. In addition, mitophagy inhibits tau pathology, and phosphorylated tau promotes mitochondrial dysfunction [6, 7]. Thus, the interaction between mitochondrial dysfunction and tau pathology may form a vicious cycle and exacerbate the development of tauopathies.

The cytoprotective PTEN-induced kinase 1 (PINK1)-parkin RBR E3 ubiquitin protein ligase (PRKN)-mediated autophagy pathway specifically eliminates damaged mitochondria (mitophagy) [8]. PINK1 is stable in the dysfunctional outer mitochondrial membrane and then phosphorylates ubiquitin and parkin. Parkin activation-mediated ubiquitination of mitochondrial outer membrane proteins is a signal for the recruitment of autophagy adaptors such as optineurin (OPTN), nuclear dot protein 52 kDa (NDP52) and sequestosome 1 (p62/SQSTM1). Then, mitochondrial autophagosomes are transported to lysosomes for degradation [9]. Neurons in the dentate gyrus of the hippocampus in 3-month-old mice exhibited high levels of mitophagy; in contrast, mitophagic activity in hippocampal neurons was significantly reduced in 21-month-old mice [10], suggesting that the expression of autophagy-related genes decreases with age [11]. The overexpression of human tau in HEK293 cells, primary hippocampal neurons, or the brains of C57 mice caused mitophagy defects [12]. Wu et al. reported that mitophagy defects in neurons increase the accumulation of damaged mitochondria, further leading to tau protein aggregation, and tau protein aggregation in turn exacerbates mitophagy defects, resulting in the loss of ATP and eventually leading to neuronal death in the brain [13].

[1]Department of Pharmacology, Shenyang Pharmaceutical University, Shenyang 110016, China
Correspondence: Peng Liu (pengliu@syphu.edu.cn) or Li-bo Zou (libozou@163.com)

Received: 13 July 2021 Revised: 27 October 2021 Accepted: 28 October 2021
Published online: 10 December 2021

The balance of mitochondrial fission and fusion dynamics is a key factor that regulates mitochondrial shape, size, and number and mediates correct mitochondrial shape and distribution, thus allowing for the needs of high-energy cells to be met [14]. Mitochondrial fusion is mainly mediated by mitochondrial fusion protein 1 (MFN1), mitochondrial fusion protein 2 (MFN2), and optic nerve atrophy protein 1 (OPA1). Mitochondrial fission is regulated by dynamic associated protein 1 (Drp1), fission protein 1 (FIS1), and mitotic factor [15]. In patients with mild cognitive impairment (MCI) (the precursor stage of AD), mitochondrial dysfunction is accompanied by high levels of ROS production, a dynamic imbalance in mitochondrial fission and fusion, and decreased function of the lysosomal system [16]. It was found that the levels of phosphorylated tau protein, the mitochondrial fission protein Drp1 and the fusion proteins MFN1, MFN2, and OPA1 were increased in the brains of rats that were treated with okadaic acid (a PP2A inhibitor), indicating tau-dependent changes in mitochondrial dynamics [17]. Moreover, in HEK293 cells, hTau enhanced MFN1, MFN2, and OPA1 protein expression [12]. Compared with age-matched WT mice, 6-month-old hTau transgenic mice exhibited MFN1, MFN2, and OPA1 accumulation in the brain [18]. Mitochondria are the source of intracellular ROS production, and more than 90% of intracellular ROS are generated by mitochondrial oxidative phosphorylation. NFTs formed by hyperphosphorylated tau protein induce the production of cytotoxic ROS and cause neuronal apoptosis [19, 20]. Recent studies have shown that insoluble tau aggregates can induce calcium influx, trigger the production of ROS by NADPH oxidase and induce oxidative stress [21]. ROS-induced mitochondrial dysfunction further increases the production of ROS, resulting in a vicious cycle between mitochondria and ROS and ultimately causing sustained oxidative damage to cells. Oxidative stress caused by excessive ROS production is inseparable from defects in the antioxidant system. The nuclear factor E2 related factor 2 (Nrf2) pathway is an important system that defends against oxidative stress. In addition, there is evidence that Nrf2 regulates mitochondrial function and metabolism [22].

Many studies have indicated that restoring neuronal PINK1 function could decrease Aβ levels in transgenic APP mice [23], but data describing the relationship between tau and PINK1-mediated mitophagy are limited. The expression of PINK1 and Parkin was found to be significantly decreased in HEK293 cells transfected with a plasmid expressing human wild-type full-length tau [12]. PINK1-mediated mitophagy was shown to reduce the level of hyperphosphorylated tau in SH-SY5Y neuroblastoma cells overexpressing 2N4R, 1N4R, and 2N3R tau and enhance memory in a tau *Caenorhabditis elegans* model and a 3 × Tg-AD mouse model [6]. However, there is no specific animal model of tau hyperphosphorylation to study the relationship between PINK1-mediated mitophagy and tau hyperphosphorylation. GSK-3β, PKA, and CaMKII are the main protein kinases that induce tau phosphorylation and contribute to cognitive dysfunction in AD. In this study, we investigated the simultaneous regulation of mitophagy, mitochondrial dynamics, and Nrf2 signaling and sought to determine whether increasing PINK1 expression could ameliorate tau hyperphosphorylation, mitochondrial dysfunction, and oxidative stress induced by forskolin and provide some insights and strategies for the treatment of AD.

MATERIALS AND METHODS

Animals

Four-month-old PINK1-knockout rats (PINK1$^{-/-}$, male, 250–280 g, SD background) were obtained from Beijing Biocytogen Co., Ltd. Age-matched SD rats (male, 250–280 g) were procured from Liao Ning Chang Sheng Biotechnology Co., Ltd. The rats were divided into six groups with ten rats in each group: AAV-GFP group, FSK/AAV-GFP group, PINK1$^{-/-}$ group, FSK/PINK1$^{-/-}$ group, AAV-PINK1 group, and FSK/AAV-PINK1 group. All rats were fed a normal light diet and were allowed to freely consume water and food. All experimental procedures were performed in accordance with the laws and regulations of the People's Republic of China for the use and care of laboratory animals, as well as the guidelines formulated by the Laboratory Animal Research Institute of Shenyang Pharmaceutical University.

Adeno-associated virus gene delivery and ICV injection of FSK

The construction and packaging of the adeno-associated viral overexpression vector was performed by Obio Technology Corp., Ltd. (Shanghai, China). PINK1 overexpression was induced by tail vein injection of the adeno-associated viral vector pAAV-CMV-PINK1-P2A-EGFP-3FLAG (AAV-PINK1), and pAAV-CMV-MCS-EGFP-3FLAG was used as the negative control (AAV-GFP). ICV injection was carried out 6 weeks after tail vein injection of the adenoviral vector. Rats were anesthetized with 2.5% Avertin (T48402, Sigma–Aldrich, USA) by i.p. injection, and the head was then fixed in a stereotaxic instrument with the rat in the supine position. The coordinates of the injection site were determined according to the stereotaxic Paxinos and Watson Atlas of the rat brain and the literature. The coordinates of the lateral ventricle were as follows: 0.8 mm posterior to the bregma, 1.5 mm lateral to the sagittal suture, and 4.0 mm ventral. Rats were injected with FSK (80 μM, 40 μL) or an equal volume of vehicle in the lateral ventricle [23, 24].

Y-maze test

The test was performed 48 h after FSK injection. The experiment was conducted in a Y-shaped maze composed of three identical wooden arms that were 40 cm long, 24 cm high, and 10 cm wide. During the experiment, each rat was allowed to move freely in the maze for 8 min, and the number of arms entered and the sequence in which the arms were entered were recorded. Entry into the three different arms in succession was defined as a correct alternative reaction. The spontaneous alternation rates of rats in each group were calculated as follows: alternation % = number of successful alternations/(total number of entries − 2) × 100.

Western blotting and antibodies

After the Y-maze test, hippocampal tissues were vigorously homogenized in 100 μL of RIPA buffer (with proportional amounts of a phosphatase inhibitor and protease inhibitor) per 10 mg of tissue. After ultrasonic homogenization, the supernatant was centrifuged at 12,000 × *g* for 15 min at 4 °C, and the sample was diluted and denatured in a water bath at 100 °C for 5 min. Aliquots of 25–30 μg of protein per lane were separated on 8%–12% SDS polyacrylamide gels and transferred to polyvinylidene difluoride membranes (Millipore). Then, 5% skim milk was used to block the membranes for 1 h at room temperature, and the membranes were then incubated with the corresponding primary antibodies overnight at 4 °C. Primary antibodies specific for the following proteins were used: SYP (Wanleibio, WL03058), PSD95 (Abcam, ab76115), NeuN (Abcam, ab104224), OXPHOS (Abcam, ab110413), PINK1 (Proteintech, 23274–1-AP), Parkin (Cell Signaling Technology, 2132 S), Drp1 (Abcam, ab56788), MFN1 (Abcam, ab57602), MFN2 (Abcam, ab56889), OPTN (Proteintech, 10837–1-AP), OPA1 (Abcam, ab42364), LC3 (Sigma, L7543), VDAC1 (Wanleibio, WL02790), β-actin (Santa Cruz Biotechnology, sc-47778), Tau Ser214 (Abcam, ab170892), Tau Ser396 (Abcam, ab109390), Tau Ser199/202 (Invitrogen, 44–768 G), Tau5 (Invitrogen, AHB0042), PI3K Tyr467 (Sigma, SAB4504314), PI3K (Cell Signaling Technology, 4257), GSK3β Ser9 (Cell Signaling Technology, 5558), GSK3β (Wanleibio, WL01456), AKT Ser473 (Proteintech, 66444–1-Ig), AKT (Wanleibio, WL0003b), HO1 (Abcam, ab68477), NQO1 (Abcam, ab80588), Nrf2 (Abcam, ab137550), and Lamin B1 (Proteintech,

12987–1-AP). Mitochondrial LC3 was isolated from total mitochondrial proteins according to the instructions of the Tissue Mitochondrial Separation Kit (Beyotime, C3606), and the corresponding mitochondrial reference protein VDAC1 was used. Cytoplasmic and nuclear proteins were extracted according to the instructions of the Nuclear and Cytoplasmic Extraction Kit (Cwbiotech, CW0199S). The membrane was washed in PBS 3 times for 10 min each and was then incubated with the corresponding HRP-conjugated secondary antibody at room temperature for 1 h. An enhanced chemiluminescence (ECL, Advanta) kit was used to amplify the signals. Band densities were determined using Image-Pro Plus analysis software (version 6.0; Media Cybernetics, Baltimore, MD).

Measurement of complex IV enzymatic activity

The WB results showed that only the expression of mitochondrial oxidative phosphorylation complex IV significantly changed. Therefore, we measured the enzymatic activity of CIV. The Complex IV Enzyme Activity Microplate Assay Kit (Abcam, ab109911) was used to rapidly and simply evaluate the activity of cytochrome *c* oxidase. Briefly, 50 μg of brain tissue homogenate was prepared, the protein concentration was adjusted to 5 mg/mL, the reaction was initiated by adding an appropriate amount of cytochrome *c* substrate solution, and the mixture was incubated at room temperature for 3 h. Then, a plate reader (Thermo Fisher, Varioskan Flash) was set to the kinetic program, and the absorbance at 550 nm was measured at 30 °C for 120 min at intervals of ~1 min.

Measurement of ATP levels

The level of ATP was determined with an ATP Bioluminescence Assay Kit (Roche, 11699709001) according to the manufacturer's instructions. Hippocampal tissue was removed from the −80 °C freezer, added to the appropriate amount of lysis buffer, incubated at 4 °C for 1 h, and centrifuged at 12,000 × *g* for 20 min. The supernatant was added to a 96-well plate, and the *OD* value was measured at 562 nm.

Estimation of oxidative stress

Approximately 30 mg of frozen brain tissue was removed from the −80 °C freezer and homogenized in 90 μL of ice-cold physiological saline per 10 mg of tissue. The brain homogenate was centrifuged at 2000 × *g* for 20 min at 4 °C, and the supernatant was collected for further analysis. The protein concentration of the brain homogenate was determined by a BCA protein assay kit. The activities of glutathione peroxidase (GSH-PX), total superoxide dismutase and nitric oxide (NO) synthase (NOS) and the levels of malondialdehyde (MDA) and NO in brain homogenate supernatant were examined according to the instructions provided by the respective assay kits (Nanjing JianCheng Bio). The absorbance values were measured by a plate reader (Thermo Fisher, Varioskan Flash).

Immunofluorescence microscopy

Rat brains were fixed for more than 24 h in 4% paraformaldehyde (PFA) in PBS (pH 7.4) at 4 °C. For single immunofluorescence staining (PINK1) or double immunofluorescence staining (NeuN and MAP2), brain slices (5 μm) were incubated at 60 °C for 3 h. Next, the slices were subjected to antigen retrieval by being boiled in citrate buffer and heated in a microwave for 20 min. Then, the slices were washed in PBS three times and blocked in 5% goat serum containing 0.1% Triton X-100 for 1 h at 37 °C. Afterward, the slices were incubated with primary antibodies against PINK1 (1:50, Proteintech, 23274–1-AP), NeuN (1:3000, Abcam, ab104224) and MAP2 (1:300, Proteintech, 17490–1-AP) overnight at 4 °C. The next day, the slices were incubated at room temperature for 20 min and washed with PBS 6 times for 5 min each prior to being incubated for 1 h at 37 °C with the following secondary antibodies: TRITC-conjugated goat anti-rabbit IgG (H + L) (1:300, ProteinTech, China) or FITC-conjugated donkey anti-mouse IgG (H + L) (1:300, ProteinTech, China). Then, the brain slices were sealed with an anti-fluorescence quenching blocking agent containing DAPI. Finally, the specimens were examined under a fluorescence microscope (Nikon, Japan). Image acquisition was completed within parallel experiments and with the same exposure times. The numbers of NeuN-positive cells in the cerebral cortex and hippocampus were determined using ImageJ software. The percentage of the MAP2-positive area was determined using Image-Pro Plus 7.0 software (Media Cybernetics, Silver Spring, MD).

Transmission electron microscopy

We perfused the apex of the rat heart with 2% PFA and 2.5% glutaraldehyde buffer and then fixed the hippocampal CA1 area in 1 mm^3 of ice-cold electron microscopy fixative for 24 h. The samples were washed three times with PBST (0.1 M, pH 7.4) for 15 min each and then fixed with 1% osmic acid for 3 h. After being washed in PBST, the samples were immersed in 50%, 70%, 90% gradient ethanol and acetone for dehydration, embedded in araldite and polymerized, and 70 nm ultrathin slices were prepared by an LKB-1 slicer. The slices were stained with uranyl acetate and lead citrate and then examined at 80 kV under a transmission electron microscope (JEM-1200EX, JEOL, Tokyo, Japan).

Statistical analysis

The results are expressed as the mean ± standard error of the mean (SEM). Statistical analysis was performed using IBM SPSS Statistics 21.0 (Statistical Package for the Social Sciences, Chicago, IL, USA). One-way analysis of variance (ANOVA) and Fisher's LSD multiple comparison test (for data with homogeneity of variance) or Dunnett's T3 test (for data with heterogeneity of variance) were used to determine statistical significance. A *t* test was used to compare differences between two groups. Statistical significance was assumed when $P < 0.05$.

RESULTS

PINK1 overexpression alleviates spatial working memory impairments in ICV-FSK rats

Previous studies reported that ICV injection with the PKA activator FSK-induced spatial memory deficits in rats in the Morris water maze test 24–72 h after injection [24]. The most significant change was seen at 48 h. In this study, we used the Y-maze test to evaluate the spatial working memory of rats 48 h after ICV FSK injection (Fig. 1a). As shown in Fig. 1b, no significant differences in the total number of arm entries were observed among the groups, which indicated that although mutated PINK1 is a Parkinson's disease-related gene, the PINK1$^{-/-}$ rats used in this study did not exhibit motor dysfunction at 4 months of age. By eliminating the interference of motor dysfunction, we more accurately evaluated the effect of PINK1 knockout on Aβ-induced spatial working memory impairment. In the test, FSK/AAV-GFP rats and FSK/PINK1$^{-/-}$ rats showed similar performance, but FSK/AAV-PINK1 rats exhibited increased alternation behavior compared to FSK/AAV-GFP rats, which demonstrated that increasing PINK1 expression alleviated spatial working memory impairments in ICV-FSK rats (Fig. 1c).

PINK1 overexpression attenuates neuronal loss and synaptic damage in the hippocampus of ICV-FSK rats

Western blot analysis confirmed that hippocampal extracts from PINK1-transduced rats showed dramatic overexpression of PINK1 compared to those of rats that were transduced with the GFP vector (Fig. 2a, b). Compared with that in FSK/AAV-GFP rats, PINK1 expression in FSK/AAV-PINK1 rats was significantly elevated. In

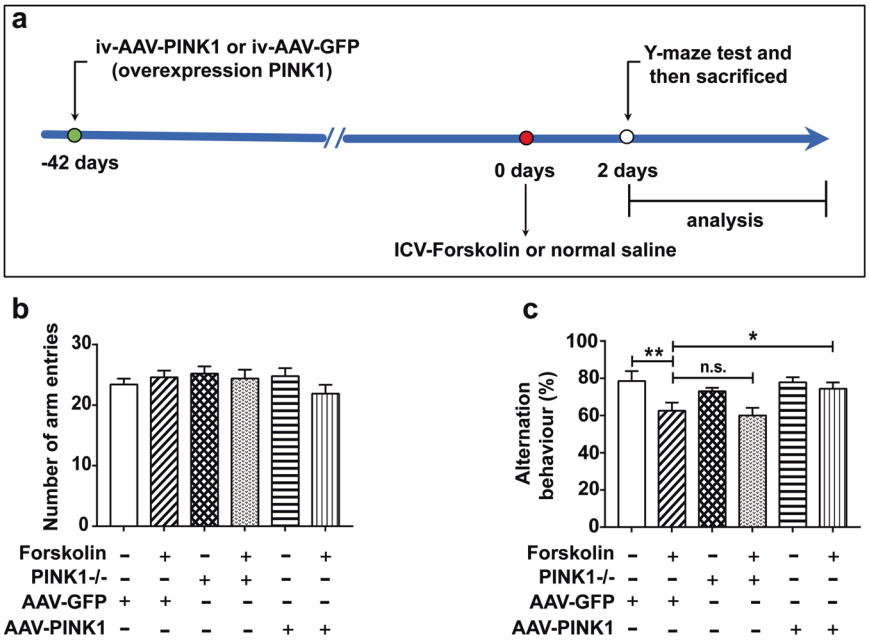

Fig. 1 PINK1 overexpression alleviates spatial working memory impairment in ICV-FSK rats. a Schematic diagram of the experimental design. The Y-maze test was performed 48 h after ICV FSK injection. **b** Number of arm entries in the Y-maze test in each group. **c** Alternation behavior in the Y-maze test in each group. The data are expressed as the mean ± SEM; $n = 10$ for each group, $^{*}P < 0.05$, $^{**}P < 0.01$.

addition, the confocal imaging results were consistent with the immunoblotting results (Fig. 2c).

Double immunofluorescence staining of NeuN (a neuronal marker, green) and MAP2 (a dendrite marker, red) was used to evaluate changes in NeuN and MAP2 in the cerebral cortex and hippocampal region. In FSK/AAV-GFP rats, the numbers of NeuN-positive cells showed marked reductions, and the percentage areas of MAP2-positive cells also robustly decreased in the cerebral cortex, hippocampal CA1, and dentate gyrus regions compared to those in AAV-GFP rats. PINK1 overexpression dramatically reduced neuronal loss in the corresponding area compared to that in FSK/AAV-GFP rats (Fig. 2d–g). The change in NeuN expression in the hippocampus was similar, as shown by Western blot analysis (Fig. 2h, i). The neurobiological basis of learning and memory formation depends on changes in synaptic plasticity. SYP and PSD95 are the core proteins in the construction of synaptic structures. It has been reported that PINK1 overexpression can improve synaptic function and reduce synaptic damage in mAPP mice [25]. Our results showed that compared with that in the AAV-GFP group, the expression of SYP and PSD95 in the FSK/AAV-GFP group was significantly decreased, and a greater decrease was observed in the FSK/PINK1$^{-/-}$ group. This decrease was prevented by PINK1 overexpression (Fig. 2h, i), suggesting that increasing PINK1 expression alleviated neuronal loss and synaptic injury induced by ICV-FSK injection in rats.

PINK1 overexpression alleviates tau hyperphosphorylation induced by ICV FSK injection by restoring the PI3K/Akt/GSK3β pathway

To explore whether mitochondrial defects could exacerbate tau hyperphosphorylation and whether PINK1 overexpression could reduce the accumulation of hyperphosphorylated tau induced by FSK, we analyzed the level of tau that was hyperphosphorylated at Ser214, Ser396, and Ser202. Compared to AAV-GFP rats, FSK/AAV-GFP rats showed higher levels of tau hyperphosphorylation at all three sites, and these increases were enhanced by PINK1 knockout and reduced by PINK1 overexpression (Fig. 3a, b), suggesting that PINK1 overexpression reduced the FSK-induced accumulation of hyperphosphorylated tau. GSK3β is an important protein kinase that regulates tau hyperphosphorylation in the brains of AD patients. PI3K and Akt are upstream kinases that phosphorylate GSK3β at Ser9 and inhibit GSK3β activity [26]. We examined whether PINK1 was involved in the regulation of tau phosphorylation through the PI3K/Akt/GSK3β signaling pathway. Decreased levels of Akt phosphorylation at Ser473 (the activated form), GSK3β phosphorylation at Ser9 (the inactivated form) and PI3K phosphorylation at Tyr467 were observed in FSK/AAV-GFP rats compared to AAV-GFP rats. These effects were reversed by PINK1 overexpression (Fig. 3c–f). There were no obvious differences in the levels of total GSK3β, Akt, and PI3K between the groups (Fig. 3g). Taken together, these results suggest that the inhibitory effect of PINK1 on tau hyperphosphorylation may be mediated by the PI3K/Akt/GSK3β signaling pathway.

PINK1 overexpression regulates mitochondrial ultrastructure, OXPHOS subunit abundance, and mitochondrial fission/fusion in the hippocampus of ICV-FSK rats

Normal mitochondrial structure is crucial for maintaining mitochondrial function. Our investigation showed that the mitochondrial structure in the CA1 area of the hippocampus in the control group was complete, the matrix was uniform, and the cristae were arranged neatly and tightly. In the AAV-GFP/FSK group and PINK1$^{-/-}$ group, most of the mitochondria were abnormal in morphology, the cristae were broken, and matrix density was lost. The mitochondria in the FSK/PINK1$^{-/-}$ group were swollen and vacuolated, and the cristae were completely lost. PINK1 overexpression ameliorated FSK-induced mitochondrial structural damage, and the results showed that the mitochondrial structure in FSK/AAV-PINK1 rats was complete, the outer membrane and cristae were clear, and there was reduced vacuolization and cristae loss in mitochondria (Fig. 4a). The assembly and efficiency of the mitochondrial oxidative phosphorylation (OXPHOS) complex (CI-CV) are determined by the inner membrane structure of mitochondria [27], which links mitochondrial morphology with function [28]. Western blot analysis showed that there were no significant changes in the expression of CI, CII, or CIII among the groups. The expression and enzymatic activity of CIV significantly increased (Fig. 4b–d), while ATP levels (Fig. 4e) significantly

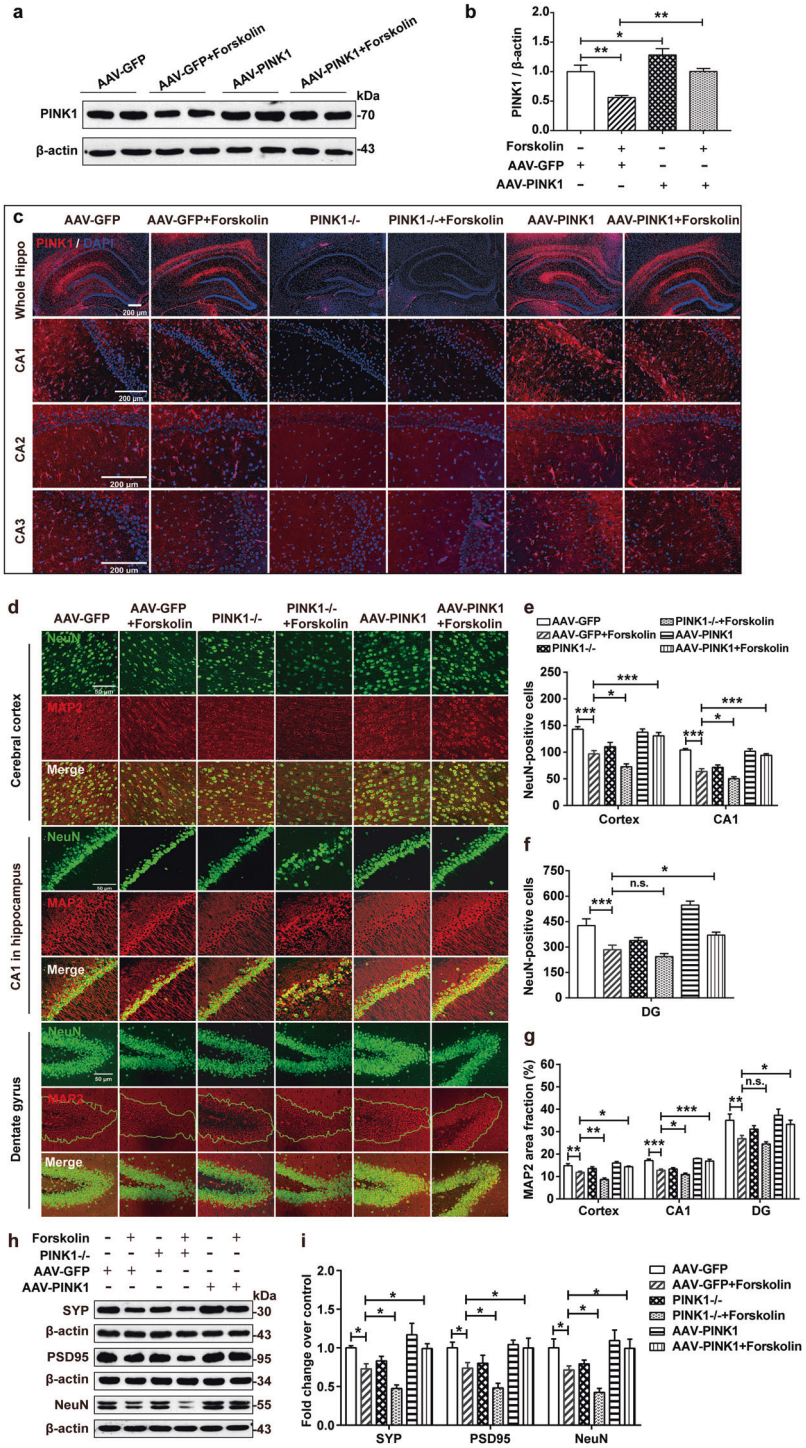

Fig. 2 PINK1 overexpression attenuates neuronal loss and synaptic damage in the hippocampus in ICV-FSK rats. a Immunoblot analysis of hippocampal tissue with antibodies against PINK1. **b** Quantification of the PINK1 band densities. **c** Representative images of whole rat hippocampal (whole Hippo) and rat hippocampal CA1, CA2, and CA3 sections showing PINK1 immunofluorescence. Scale bars: 200 μm. **d** Representative immunofluorescence images of NeuN and MAP2 labeling in the cerebral cortex and the hippocampal CA1 and dentate gyrus (DG). Scale bars: 50 μm. **e** The number of NeuN-positive cells in the cerebral cortex and hippocampal CA1 region in the different groups. **f** The number of NeuN-positive cells in the dentate gyrus in the different groups. **g** The percentage areas of MAP2-positive cells in the cerebral cortex, hippocampal CA1 region, and dentate gyrus (DG) in the different groups (the percentage area of MAP2-positive cells in the DG was only measured in the green closed area). **h** Immunoblot analysis of hippocampal tissue with antibodies against SYP, PSD95, and NeuN. **i** Quantification of the band densities of SYP, PSD95, and NeuN. The data are expressed as the mean ± SEM; $n = 5$ for each group, $^{*}P < 0.05$, $^{**}P < 0.01$, $^{***}P < 0.001$.

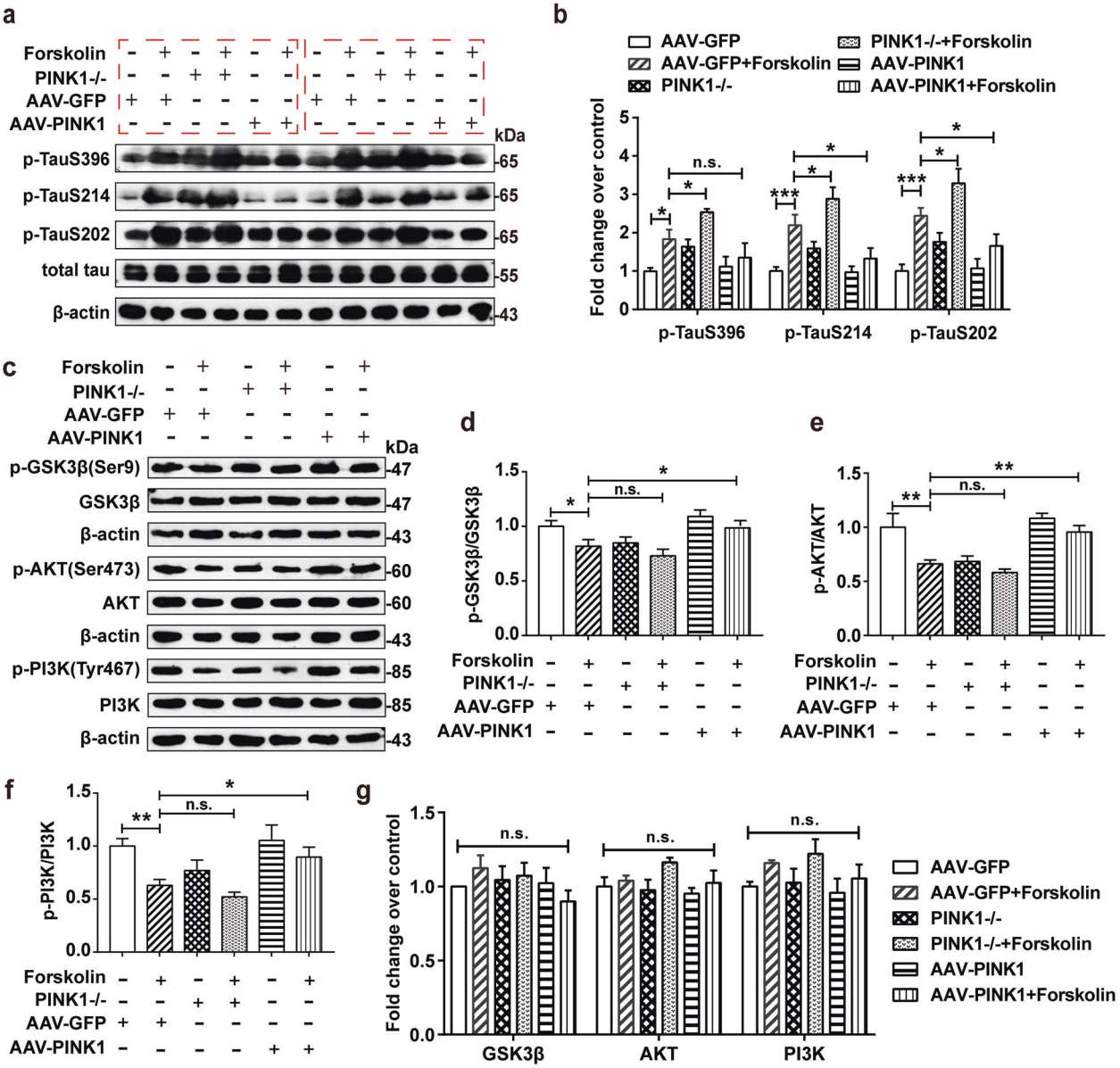

Fig. 3 PINK1 overexpression alleviates FSK-induced tau hyperphosphorylation by restoring PI3K/Akt/GSK3β pathway activity. **a** Immunoblot analysis of hippocampal tissue with antibodies against Tau S396, Tau S214, Tau S202, and Tau5. **b** Quantification of the band densities of Tau S396, Tau S214, and Tau S202. **c** Immunoblot analysis of hippocampal tissue with antibodies against p-GSK3β (Ser9), p-AKT (Ser473), p-PI3K (Tyr467), GSK3β, AKT, and PI3K. **d**–**g** Quantification of the band densities of p-GSK3β (Ser9), p-AKT (Ser473), p-PI3K (Tyr467), GSK3β, AKT, and PI3K. The data are expressed as the mean ± SEM; $n = 5$ for each group, $^{*}P < 0.05$, $^{**}P < 0.01$, $^{***}P < 0.001$.

decreased in FSK/AAV-GFP rats compared to AAV-GFP rats. PINK1 knockout exacerbated the FSK-induced decrease in ATP. This change was reversed by PINK1 overexpression.

Mitochondria are in a dynamic balance of fission and fusion to maintain morphology and function [20]. The key proteins that regulate mitochondrial fission and fusion include the fission protein Drp1, mitochondrial inner membrane fusion protein OPA1, and mitochondrial outer membrane fusion protein MFN1/2 [29]. There was no obvious change in the expression of the mitochondrial fission protein Drp1 among the groups (Fig. 4f, g). We found that the amount of MFN2 (but not MFN1) was markedly increased in FSK/AAV-GFP rats compared to AAV-GFP rats. Upregulation of MFN1 and MFN2 was observed in the hippocampus of FSK/PINK1$^{-/-}$ rats compared with FSK/AAV-GFP rats. PINK1 overexpression reversed the increase in MFN1 and MFN2 expression in the rat hippocampus. Compared with that in FSK/AAV-GFP rats, the expression of OPA1 was slightly but not significantly decreased in AAV-PINK1 rats (Fig. 4f, g).

These results strongly indicate that tau hyperphosphorylation is related to changes in mitochondrial dynamics and OXPHOS structure and function. Increasing PINK1 expression reverses the abnormal changes in mitochondrial dynamics and OXPHOS subunits induced by tau hyperphosphorylation in ICV-FSK rats.

PINK1 overexpression activates the mitophagy signaling pathway in the hippocampus of ICV-FSK rats

Defective mitophagy plays a critical role in AD development and progression [6]. We found that the expression of the mitophagy receptors Parkin, OPTN. and NDP52 was significantly decreased in the hippocampus of FSK/AAV-GFP rats compared with AAV-GFP rats. Interestingly, compared with that in FSK/AAV-GFP rats, the expression of these proteins in FSK/PINK1$^{-/-}$ rats was significantly

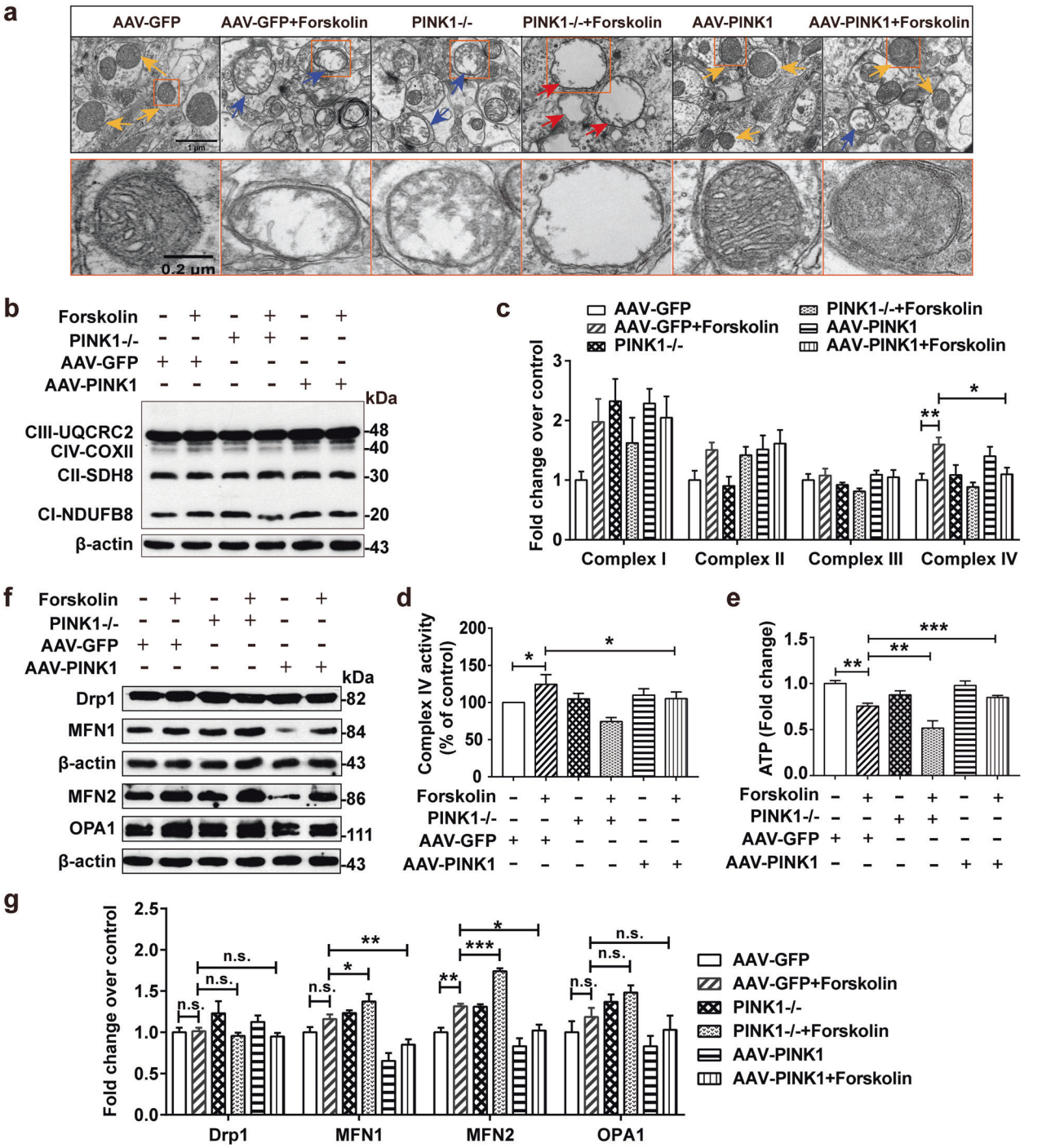

Fig. 4 PINK1 overexpression regulates mitochondrial ultrastructure, OXPHOS subunit abundance, and mitochondrial fission/fusion in the hippocampus in ICV-FSK rats. a Representative images of mitochondrial ultrastructure in the hippocampal CA1 region. Scale bar: 1 μm. Zoomed scale bar: 0.2 μm. The yellow arrow indicates dark mitochondria with uniform matrices filled with densely packed and regularly distributed cristae, the blue arrow indicates mitochondria with disrupted cristae and lost matrix density, and the red arrow indicates swollen mitochondria with vacuolization and the complete loss of cristae. The data were obtained from two independent experiments performed in duplicate. **b** Immunoblot analysis of the hippocampus with antibodies against OXPHOS. **c** Quantification of the band densities of complex I-NDUFB8, complex II-SDH8, complex III-UQCRC2, and complex IV-COXII. **d** A Complex IV Enzyme Activity Microplate Assay Kit was used to determine the activity of cytochrome *c* oxidase. **e** The level of ATP was determined by an ATP Bioluminescence Assay Kit. **f** Immunoblot analysis of the hippocampus with antibodies against Drp1, MFN1, MFN2 and OPA1. **g** Quantification of the band densities of Drp1, MFN1, MFN2, and OPA1. The data are expressed as the mean ± SEM; $n = 5$ for each group, $^{*}P < 0.05$, $^{**}P < 0.01$, $^{***}P < 0.001$.

increased. This increase may be a compensatory self-protective response to PINK1 knockout. In contrast, PINK1 overexpression increased the expression of Parkin and OPTN in the rat hippocampus (Fig. 5a–d).

We isolated mitochondria from the hippocampus and estimated the expression levels of LC3 and p62/SQSTM1. The level of LC3-II (an autophagosome marker), which is the active form of LC3, was significantly decreased in FSK/AAV-GFP rats compared to AAV-GFP

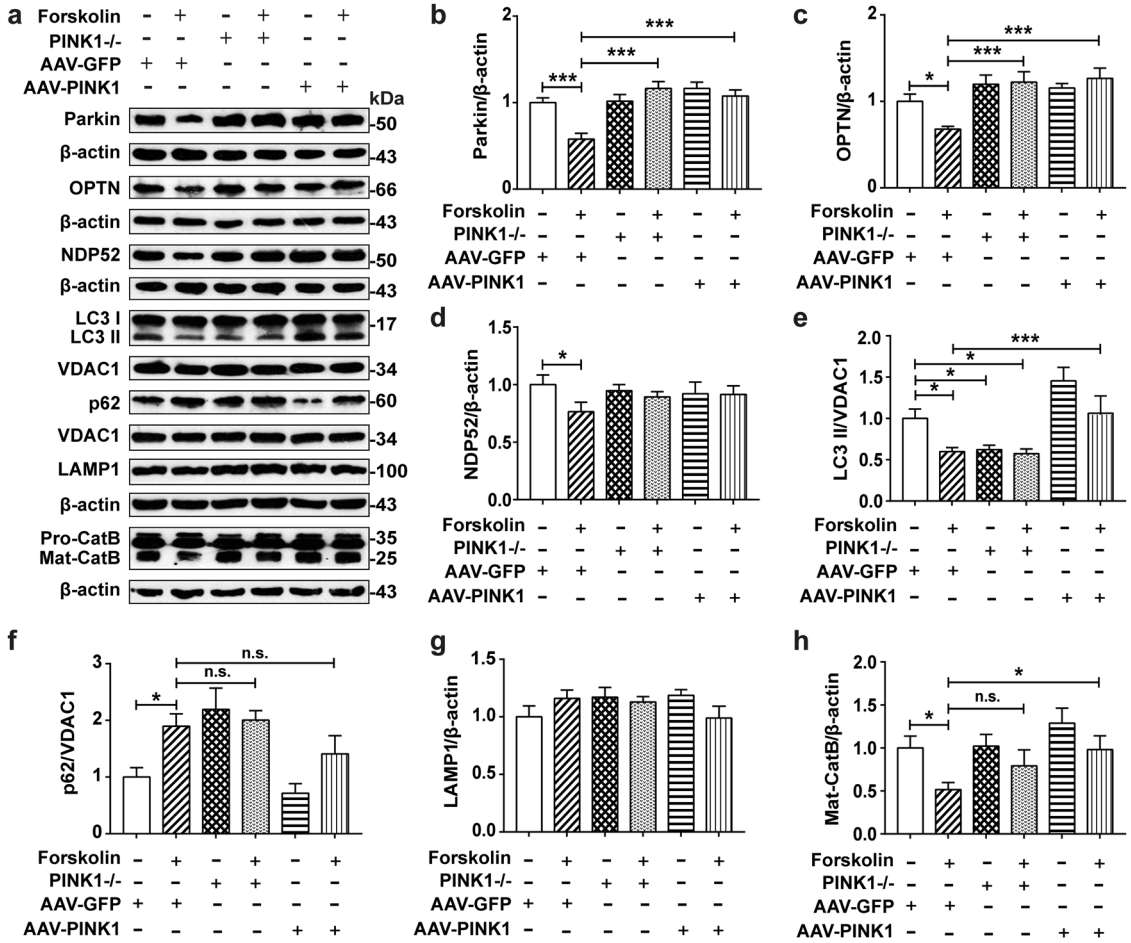

Fig. 5 PINK1 overexpression enhances mitophagy signaling pathway activity in the hippocampus of ICV-FSK rats. a Immunoblot analysis of hippocampal tissue with antibodies against mitophagy- and lysosome-related proteins. **b**–**h** Quantification of the band densities of Parkin, OPTN, NDP52, LC3II, p62, LAMP1, and Mat-CatB. The data are expressed as the mean ± SEM; $n = 5$ for each group, $^{*}P < 0.05$, $^{***}P < 0.001$.

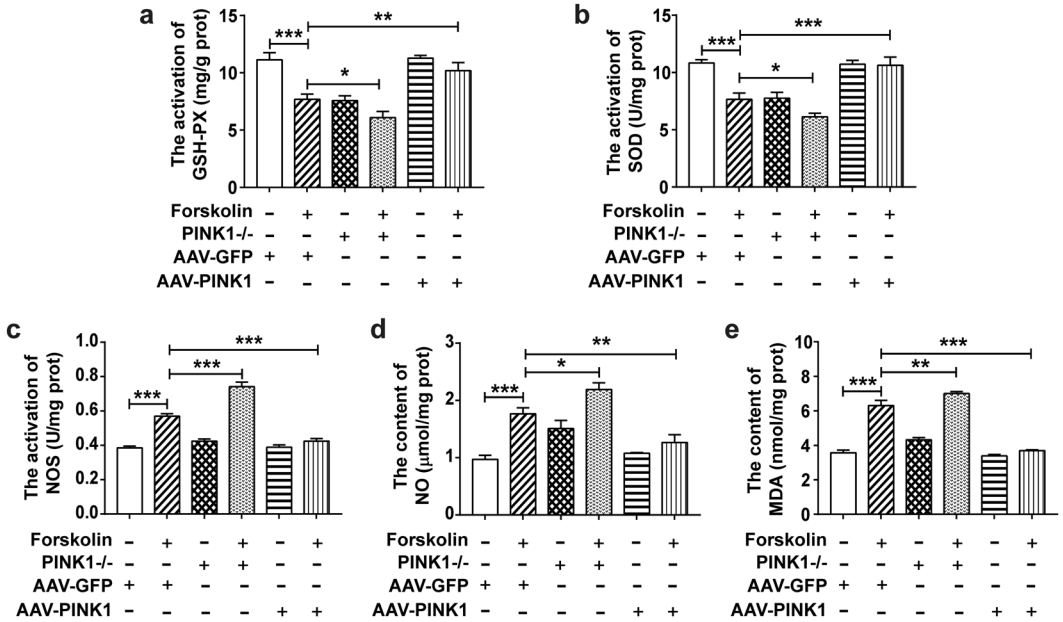

Fig. 6 PINK1 overexpression regulates the activities of SOD, GSH-PX, and NOS and the levels of MDA and NO in the hippocampus of ICV-FSK rats. a–**c** The activities of GSH-PX, SOD and NOS in the hippocampus of rats in the different groups. **d**, **e** The levels of NO and MDA in the hippocampus of rats in the different groups. The data are expressed as the mean ± SEM; $n = 5$ for each group, $^{*}P < 0.05$, $^{**}P < 0.01$, $^{***}P < 0.001$.

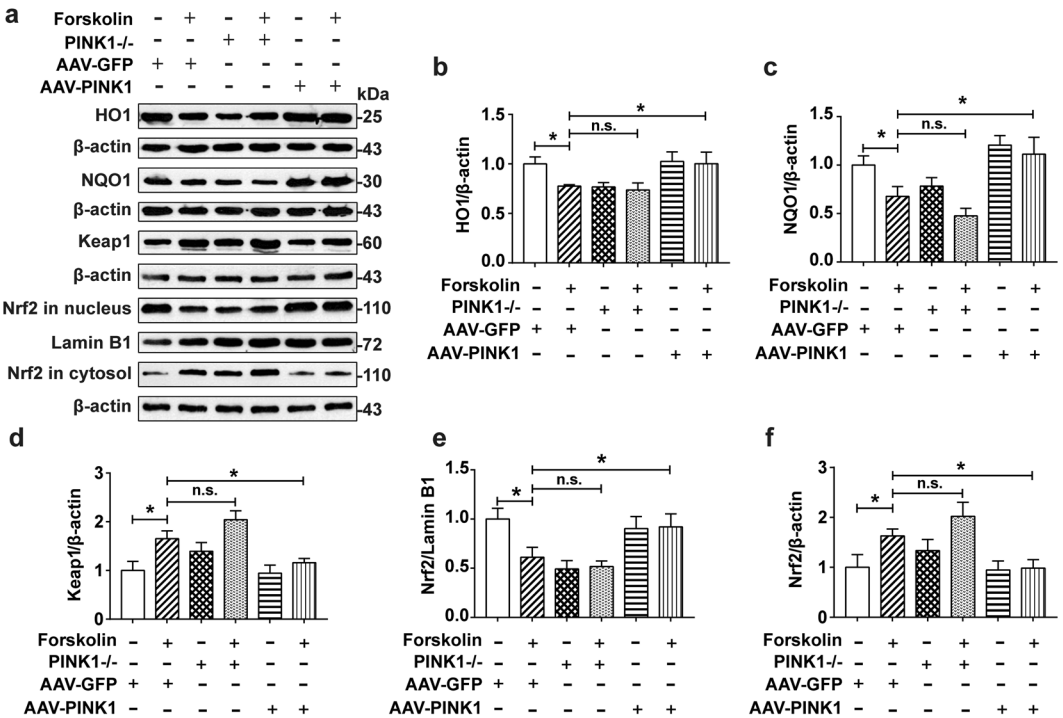

Fig. 7 PINK1 overexpression activates the Nrf2 pathway in the hippocampus in ICV-FSK rats. a Immunoblot analysis of hippocampal tissue with antibodies against HO1, NQO1, Keap1, and Nrf2. **b**–**f** Quantification of the band densities of HO1, NQO1, Keap1, and Nrf2 in the subcellular fraction. The data are expressed as the mean ± SEM; $n = 5$ for each group, $^{*}P < 0.05$, $^{**}P < 0.01$, $^{***}P < 0.001$.

rats. PINK1 overexpression significantly increased the expression of LC3II in rats (Fig. 5e). FSK injection obviously upregulated the expression of p62 (an autophagy adaptor protein) compared with that in the AAV-GFP group (Fig. 5f). Western blot analysis was also used to evaluate the expression of the lysosomal markers LAMP1 (lysosomal associated membrane protein 1) and CatB (cathepsin B, a lysosomal acidic protease). There was no dramatic difference in the expression of LAMP1 among the groups (Fig. 5g), but compared with that in the AAV-GFP group, the Mat-CatB (mature cathepsin B) level was significantly decreased in the FSK/AAV-GFP group (Fig. 5h). Moreover, FSK-induced lysosomal dysfunction was reversed by PINK1 overexpression. Accordingly, hyperphosphorylated tau inhibited mitophagy and impaired lysosomal function, and these effects were reversed by PINK1 overexpression.

PINK1 overexpression prevents oxidative stress-induced damage in the hippocampus of ICV-FSK rats

Tau hyperphosphorylation causes an imbalance in the oxidant and antioxidant systems. Pathological defects in mitophagy may be caused by mild oxidative stress resulting from mitochondrial ROS or oxidized protein aggregates [27]. The activities of GSH-PX (Fig. 6a) and SOD (Fig. 6b) in the hippocampus of FSK/AAV-GFP rats were lower than those in AAV-GFP rats, while the activity of NOS (Fig. 6c) and the levels of NO (Fig. 6d) and MDA (Fig. 6e) were higher. PINK1 knockout exacerbated oxidative stress-induced damage in rats. Compared with those in FSK/AAV-GFP rats, the activities of GSH-PX and SOD were significantly decreased, and the activity of NOS and the levels of NO and MDA were further increased in FSK/PINK1$^{-/-}$ rats. These changes in the hippocampus in AAV-FSK rats were reversed by increasing PINK1 expression. These results indicate that increased PINK1 expression/activity markedly alleviates the oxidative stress induced by ICV FSK injection in rats.

Nrf2 is a key regulatory protein of the endogenous antioxidant defense system that can activate the transcription of downstream antioxidant enzymes to respond to oxidative stress [28]. Furthermore, Nrf2 has been shown to regulate mitochondrial function and metabolism [29]. The Western blot results showed that the expression of Keap1 and cytosolic Nrf2 was upregulated, while the expression of nuclear Nrf2 and the antioxidant proteins HO1 and NQO1 was downregulated in FSK/AAV-GFP rats compared to AAV-GFP rats. As expected, compared with FSK/AAV-GFP rats, FSK/AAV-PINK1 rats showed lower expression levels of Keap1 and cytosolic Nrf2 and higher expression levels of nuclear Nrf2, HO1, and NQO1 (Fig. 7a–f). Thus, PINK1 overexpression activates the Nrf2 pathway, increases the expression of antioxidant proteins and reduces oxidative damage in the hippocampus in ICV-FSK rats.

DISCUSSION

AD is the most common cause of dementia, and in addition to Aβ, microtubule-associated protein Tau and NFTs are potential contributors to AD pathogenesis [9, 30]. The aggregation of hyperphosphorylated tau is associated with mitochondrial damage, oxidative stress and structural and functional changes in neurons in AD [31]. Effective clearance of damaged mitochondria is the key mechanism controlling mitochondrial quality. Mitophagy is an important process for the removal of damaged mitochondria [32]. In the AD brain, intracellular accumulation of wild-type full-length tau was shown to inhibit mitophagy [12]. Mitochondrial abnormalities were also observed in transgenic mice expressing a P301L tau mutant [33, 34]. The PINK1/Parkin pathway is the main pathway that mediates mitophagy. The literature reports that PINK1 overexpression extends the lifespan of *Drosophila melanogaster* and protects against cerebral ischemia in rats [35, 36]. Therefore, PINK1 activation may have a neuroprotective effect. In the current study, we provide evidence of multiple PINK1-dependent pathways that are relevant to tau pathology, oxidative stress, mitochondrial damage, neuronal loss, synaptic damage, and cognitive dysfunction in a specific rat model of tau hyperphosphorylation induced by PKA activation.

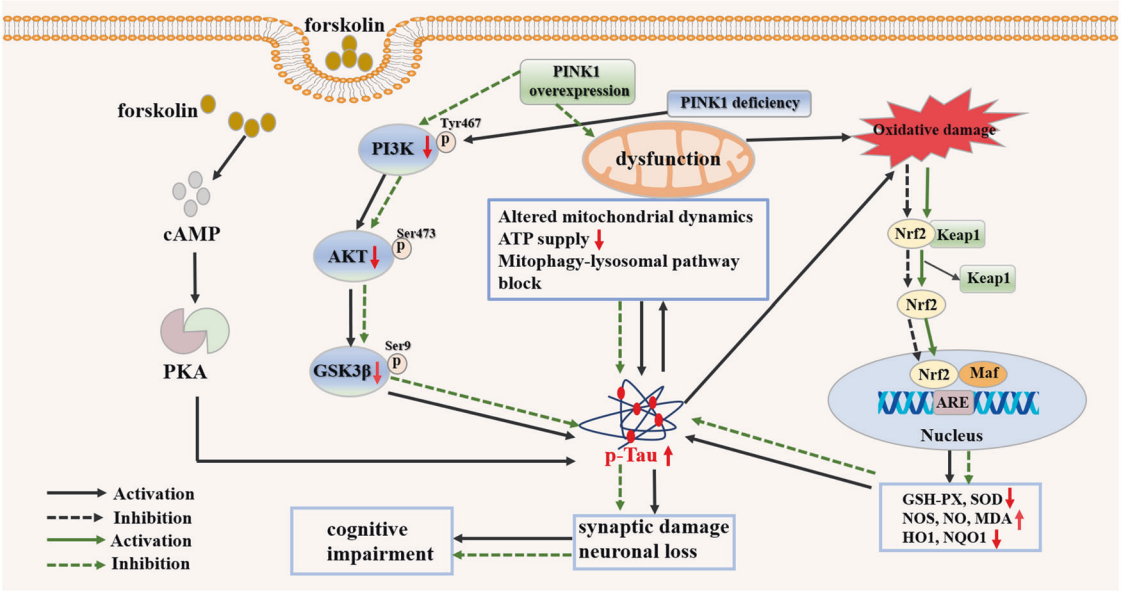

Fig. 8 Schematic diagram of the effect of PINK1 on Alzheimer's disease-like pathology induced by intracerebroventricular injection of forskolin in rats. PINK1 deficiency exacerbates ICV-FSK-induced mitochondrial dysfunction, antioxidant system damage, tau pathology, synaptic damage, and neuronal loss and ultimately enhances ICV-FSK-induced cognitive impairment in rats. Moreover, tau pathology damages mitochondria and forms a vicious cycle. Importantly, PINK1 overexpression alleviates tau hyperphosphorylation by restoring PI3K/Akt/GSK3β pathway activity, reversing the abnormal changes in mitochondrial dynamics, defective mitophagy, and ATP decrease in the rat hippocampus, activating the Nrf2 pathway to increase the expression of antioxidant proteins and reduce oxidative damage.

More importantly, we also found that PINK1 overexpression prevented cognitive impairment and multiple tau-associated pathological changes.

A study reported that intracerebroventricular injection of 80 μmol of FSK induced tau hyperphosphorylation in the rat brain and resulted in memory impairment [24]. We used 4-month-old PINK1$^{-/-}$ rats, which have normal motor and cognitive functions (unpublished data), to investigate the relationship between PINK1 expression and AD-like pathology in a model of ICV FSK injection. PINK1 knockout did not enhance ICV FSK injection-induced spatial working memory deficits in rats, and PINK1 overexpression improved the performance of rats in the Y-maze test. Imaging studies and postmortem examinations of AD patients showed significant decreases in brain volume and the number of neurons, indicating severe neuronal loss [37, 38]. We found that the number of cells positive for the neuron marker NeuN was significantly decreased in the cerebral cortex and hippocampal region in FSK/AAV-GFP rats. The injection of AAV-PINK1 prevented the loss of neurons. The percentage areas of MAP2-positive cells and the expression levels of the synaptic marker proteins PSD95 and SYP were also decreased in the hippocampus after ICV-FSK injection, and these effects were inhibited by AAV-PINK1 injection. PINK1 overexpression alleviated synaptic damage and neuronal loss in the cerebral cortex and hippocampus in ICV-FSK rats.

Evidence has shown that PINK1 expression is related to amyloid pathology [25]. However, there is no specific animal model of tau hyperphosphorylation to study the relationship between PINK1-mediated mitophagy and tau hyperphosphorylation. Protein kinases, such as GSK-3β, PKA, and CaMKII, can induce tau phosphorylation and contribute to cognitive dysfunction in AD. Therefore, we used an ICV-FSK (a PKA activation) rat model to induce tau hyperphosphorylation, which eliminated Aβ interference, and investigated whether PINK1 expression was also related to tau pathology. We found that PINK1 deficiency increased the accumulation of hyperphosphorylated tau, and PINK1 overexpression decreased hyperphosphorylated tau accumulation. Abnormal hyperphosphorylation of tau is thought to be caused by an imbalance in specific tau kinase and phosphatase activities [39, 40]. Among the two major categories of protein kinases, PKA, a nonproline-directed protein kinase, plays an important role in the hyperphosphorylation of the AD-associated tau protein. Previous studies have shown that PKA can be activated by FSK and that injection of FSK into the rat brain results in tau hyperphosphorylation and spatial memory impairment [41–43]. GSK3β and PKA have a positive synergistic effect; in other words, tau protein that is first phosphorylated by PKA is more easily hyperphosphorylated by GSK3β [23, 44]. PI3K/Akt are the upstream kinases that phosphorylate GSK3β at Ser9 and inhibit GSK3β activity [26]. In our study, decreased levels of Akt phosphorylated at Ser473 (the activated form), GSK3β phosphorylated at Ser9 (the inactivated form) and PI3K phosphorylated at Tyr467 were observed in FSK/AAV-GFP rats. These effects were reversed by PINK1 overexpression. These results suggest that the inhibitory effect of PINK1 on tau phosphorylation may be mediated by the PI3K/Akt/GSK3β signaling pathway.

Mitochondria are the main source of cellular energy production in the form of ATP via OXPHOS [40]. Mitochondrial complexes I, II, III, and IV, which collectively compose the electron transport chain and ATP synthase (complex V), are embedded in the inner mitochondrial membrane (IMM) [45]. Previous studies have reported increased OXPHOS gene expression in the hippocampus in MCI patients [46]. The mRNA levels of OXPHOS complexes III and IV were increased in brain specimens from patients with both early and defined AD [47]. Hirai et al. also showed that pyramidal neurons exhibited increased levels of mtDNA and cytochrome oxidase (complex IV) in the AD hippocampus [48]. These results are consistent with our results. Abnormally hyperphosphorylated tau significantly increased the expression and activity of complex IV, but there were no significant changes in the expression or activity of complexes I, II, and III. PINK1 overexpression restored the level of complex IV. We also found that PINK1 deficiency exacerbated the reduction in ATP induced by hyperphosphorylated tau, and this effect was prevented by PINK1 overexpression. Fission and fusion are two major processes associated with mitochondrial dynamics. The balance of mitochondrial fission and fusion regulates the number, shape, and size of mitochondria. To

investigate the effect of PINK1 and hyperphosphorylated tau on mitochondrial dynamics, we assessed the levels of Drp1 as a fission marker and OPA1, MFN1, and MFN2 as fusion markers. We found that hyperphosphorylated tau significantly increased the expression of MFN2. PINK1 deficiency enhanced the increase in MFN1 and MFN2 expression induced by hyperphosphorylated tau. However, PINK1 overexpression decreased the expression of fusion proteins. PINK1 overexpression may promote the degradation of MFN1 and MFN2 by ubiquitination. In *Drosophila* expressing human R406W tau, the brains of rTg4510 and K3 mice [49], and THY-Tau22 mice with early-stage tau pathology, elongation of the mitochondrial network was observed [20]. Overexpression of human wild-type tau (htau) increased the levels of the fusion proteins OPA1 and MFN1/2 and resulted in mitochondrial elongation [18]. Damaged and energy-deficient mitochondria can be selectively degraded by mitophagy. In AD patients with APP mutations or two copies of ApoE4, mitophagy was found to be impaired [6]. The PINK1/parkin-mediated mitophagy pathway plays an important role in the clearance of damaged mitochondria. In healthy mitochondria, PINK1 enters the IMM and is degraded by proteolytic enzymes [50]. When mitochondria are damaged, PINK1-induced parkin accumulates on mitochondria and then mediates VDAC1 ubiquitination and recruits mitophagy receptors and LC3. Subsequently, mitochondrial autophagosomes are degraded by lysosomes [51]. The mRNA and protein levels of PINK1, parkin, and other mitotic phagocytic and autophagic proteins were found to be decreased in AD patients and AD transgenic mice [52]. In this study, abnormally hyperphosphorylated tau inhibited mitophagy and impaired lysosomal function, as indicated by decreased expression of mitochondrial LC3II, the accumulation of the autophagy adapter p62/SQSTM1, and decreased expression of the mitophagy receptors Parkin, OPTN, and NDP52 and the lysosomal hydrolase Cathepsin B. PINK1 overexpression rescued defective mitophagy and lysosomal dysfunction. The literature reports that silencing PINK1 impairs mitophagy but does not decrease the expression of Parkin in primary Kupffer cells or kidney cortex tissues in mice [53, 54]. Parkin upregulation could not reverse the effects of PINK1 knockdown. Therefore, PINK1 kinase activity but not Parkin or OPTN activity is crucial for PINK1/Parkin/OPTN pathway-mediated mitophagy. In this study, although there was an increase in the expression of mitophagy receptors after PINK1 knockout, the mitophagy level was still inhibited.

Accumulating evidence shows that almost all macromolecules in the brains of AD patients have increased oxidative damage [55]. Approximately 90% of ROS are generated by mitochondria, and excessive ROS accumulation results in oxidative stress. The increase in oxidative stress may be both the cause and consequence of mitochondrial dysfunction [56]. Nrf2 is a key regulatory protein in the endogenous antioxidant defense system. Under oxidative stress conditions, Nrf2 translocates to the nucleus, activates antioxidant response elements, and promotes the expression and activity of downstream antioxidant proteins (such as HO1 and NQO1) and antioxidant enzymes (such as SOD and GSH-PX) [57]. The level of MDA, a product of lipid peroxidation, is increased in many brain regions affected by AD and MCI [58], while the glutathione level is decreased in an AD-dependent manner [59]. In our study, the nuclear level of Nrf2 was decreased in the hippocampus of FSK-induced AD rats; the expression or activity of the downstream antioxidant enzymes HO-1, NQO1, SOD, and GSH-PX was decreased; and the activity of NOS and the levels of NO and MDA were increased. These effects were reversed by PINK1 overexpression. In contrast, PINK1 deficiency exacerbated FSK-induced oxidative damage in the hippocampus of AD rats.

In summary, the results of the present study suggest that PINK1 deficiency exacerbates ICV FSK-induced tau pathology, synaptic damage, mitochondrial dysfunction and oxidative damage in this rat model of tau hyperphosphorylation. These changes were reversed by PINK1 overexpression (Fig. 8). Therefore, our data support a critical role of PINK1-mediated mitophagy in controlling mitochondrial quality, tau hyperphosphorylation, and oxidative stress in an AD rat model.

ACKNOWLEDGEMENTS

This work was supported by the National Natural Science Foundation of China (81703494).

AUTHOR CONTRIBUTIONS

PL and LBZ conceived the project and designed the experiments. XJW performed the experiments and data analysis with the help of LQ, YFC, XFJ, and TYC. PL and XJW wrote the manuscript, and LBZ revised the manuscript.

ADDITIONAL INFORMATION

Competing interests: The authors declare no competing interests.

REFERENCES

1. Canepa E, Fossati S. Impact of tau on neurovascular pathology in Alzheimer's disease. Front Neurol. 2020;11:573324.
2. Blennow K, Chen C, Cicognola C, Wildsmith KR, Manser PT, Bohorquez SMS, et al. Cerebrospinal fluid tau fragment correlates with tau PET: a candidate biomarker for tangle pathology. Brain. 2020;143:650–60.
3. Yang Y, Wang JZ. Nature of Tau-associated neurodegeneration and the molecular mechanisms. J Alzheimers Dis. 2018;62:1305–17.
4. Swerdlow RH, Burns JM, Khan SM. The Alzheimer's disease mitochondrial cascade hypothesis: progress and perspectives. Biochim Biophys Acta. 2014;1842:1219–31.
5. Zhang L, Trushin S, Christensen TA, Bachmeier BV, Gateno B, Schroeder A, et al. Altered brain energetics induces mitochondrial fission arrest in Alzheimer's Disease. Sci Rep. 2016;6:18725.
6. Fang EF, Hou Y, Palikaras K, Adriaanse BA, Kerr JS, Yang B, et al. Mitophagy inhibits amyloid-beta and tau pathology and reverses cognitive deficits in models of Alzheimer's disease. Nat Neurosci. 2019;22:401–12.
7. Reddy PH, Oliver DM. Amyloid beta and phosphorylated Tau-induced defective autophagy and mitophagy in Alzheimer's disease. Cell. 2019;8:488.
8. Hou X, Watzlawik JO, Cook C, Liu CC, Kang SS, Lin WL, et al. Mitophagy alterations in Alzheimer's disease are associated with granulovacuolar degeneration and early tau pathology. Alzheimers Dement. 2020;17:417–30.
9. Song M, Zhao X, Song F. Aging-dependent mitophagy dysfunction in Alzheimer's disease. Mol Neurobiol. 2021;58:2362–78.
10. Sun N, Yun J, Liu J, Malide D, Liu C, Rovira II, et al. Measuring in vivo mitophagy. Mol Cell. 2015;60:685–96.
11. Castellazzi M, Patergnani S, Donadio M, Giorgi C, Bonora M, Bosi C, et al. Autophagy and mitophagy biomarkers are reduced in sera of patients with Alzheimer's disease and mild cognitive impairment. Sci Rep. 2019;9:20009.
12. Hu Y, Li XC, Wang ZH, Luo Y, Zhang XN, Liu XP, et al. Tau accumulation impairs mitophagy via increasing mitochondrial membrane potential and reducing mitochondrial Parkin. Oncotarget. 2016;7:17356–68.
13. Wu XL, Pina-Crespo J, Zhang YW, Chen XC, Xu HX. Tau-mediated neurodegeneration and potential implications in diagnosis and treatment of Alzheimer's disease. Chin Med J. 2017;130:2978–90.
14. Yamada T, Dawson TM, Yanagawa T, Iijima M, Sesaki H. SQSTM1/p62 promotes mitochondrial ubiquitination independently of PINK1 and PRKN/parkin in mitophagy. Autophagy. 2019;15:2012–8.
15. Ren L, Chen X, Chen X, Li J, Cheng B, Xia J. Mitochondrial dynamics: fission and fusion in fate determination of mesenchymal stem cells. Front Cell Dev Biol. 2020;8:580070.
16. Nikhil K, Shah K. The Cdk5-Mcl-1 axis promotes mitochondrial dysfunction and neurodegeneration in a model of Alzheimer's disease. J Cell Sci. 2017;130:3023–39.
17. Placido AI, Pereira CMF, Correira SC, Carvalho C, Oliveira CR, Moreira PI. Phosphatase 2A inhibition affects endoplasmic reticulum and mitochondria homeostasis via cytoskeletal alterations in brain endothelial cells. Mol Neurobiol. 2017;54:154–68.
18. Li XC, Hu Y, Wang ZH, Luo Y, Zhang Y, Liu XP, et al. Human wild-type full-length tau accumulation disrupts mitochondrial dynamics and the functions via increasing mitofusins. Sci Rep. 2016;6:24756.

19. Zhou H, Gong Y, Liu Y, Huang A, Zhu X, Liu J, et al. Intelligently thermoresponsive flower-like hollow nano-ruthenium system for sustained release of nerve growth factor to inhibit hyperphosphorylation of tau and neuronal damage for the treatment of Alzheimer's disease. Biomaterials. 2020;237:119822.
20. Zheng J, Akbari M, Schirmer C, Reynaert ML, Loyens A, Lefebvre B, et al. Hippocampal tau oligomerization early in tau pathology coincides with a transient alteration of mitochondrial homeostasis and DNA repair in a mouse model of tauopathy. Acta Neuropathol Commun. 2020;8:25.
21. Esteras N, Kundel F, Amodeo GF, Pavlov EV, Klenerman D, Abramov AY. Insoluble tau aggregates induce neuronal death through modification of membrane ion conductance, activation of voltage-gated calcium channels and NADPH oxidase. FEBS J. 2021;288:127–41.
22. Dinkova-Kostova AT, Abramov AY. The emerging role of Nrf2 in mitochondrial function. Free Radic Biol Med. 2015;88:179–88.
23. Liu SJ, Zhang JY, Li HL, Fang ZY, Wang Q, Deng HM, et al. Tau becomes a more favorable substrate for GSK-3 when it is prephosphorylated by PKA in rat brain. J Biol Chem. 2004;279:50078–88.
24. Tian Q, Zhang JX, Zhang Y, Wu F, Tang Q, Wang C, et al. Biphasic effects of forskolin on tau phosphorylation and spatial memory in rats. J Alzheimers Dis. 2009;17:631–42.
25. Du F, Yu Q, Yan S, Hu G, Lue LF, Walker DG, et al. PINK1 signalling rescues amyloid pathology and mitochondrial dysfunction in Alzheimer's disease. Brain. 2017;140:3233–51.
26. Wang S, He B, Hang W, Wu N, Xia L, Wang X, et al. Berberine alleviates Tau hyperphosphorylation and axonopathy-associated with diabetic encephalopathy via restoring PI3K/Akt/GSK3beta pathway. J Alzheimers Dis. 2018;65:1385–400.
27. Sun K, Jing X, Guo J, Yao X, Guo F. Mitophagy in degenerative joint diseases. Autophagy. 2020;17:2082–92.
28. Krajka-Kuźniak V, Paluszczak J, Baer-Dubowska W. The Nrf2-ARE signaling pathway: an update on its regulation and possible role in cancer prevention and treatment. Pharmacol Rep. 2017;69:393–402.
29. Holmstrom KM, Kostov RV, D-K AT. The multifaceted role of Nrf2 in mitochondrial function. Curr Opin Toxicol. 2016;1:80–91.
30. Rai SN, Singh C, Singh A, Singh MP, Singh BK. Mitochondrial dysfunction: a potential therapeutic target to treat Alzheimer's disease. Mol Neurobiol. 2020; 57:3075–88.
31. Wang W, Zhao F, Ma X, Perry G, Zhu X. Mitochondria dysfunction in the pathogenesis of Alzheimer's disease: recent advances. Mol Neurodegener. 2020;15:30.
32. Bell SM, Barnes K, De Marco M, Shaw PJ, Ferraiuolo L, Blackburn DJ, et al. Mitochondrial dysfunction in Alzheimer's disease: a biomarker of the future? Biomedicines. 2021;9:63.
33. David DC, Hauptmann S, Scherping I, Schuessel K, Keil U, Rizzu P, et al. Proteomic and functional analyses reveal a mitochondrial dysfunction in P301L tau transgenic mice. J Biol Chem. 2005;280:23802–14.
34. Rhein V, Song X, Wiesner A, Ittner LM, Baysang G, Meier F, et al. Amyloid-β and tau synergistically impair the oxidative phosphorylation system in triple transgenic Alzheimer's disease mice. Proc Natl Acad Sci USA. 2009;106: 20057–62.
35. Si H, Ma P, Liang Q, Yin Y, Wang P, Zhang Q, et al. Overexpression of pink1 or parkin in indirect flight muscles promotes mitochondrial proteostasis and extends lifespan in Drosophila melanogaster. PLoS One. 2019;14:e0225214.
36. Wen Y, Gu Y, Tang X, Hu Z. PINK1 overexpression protects against cerebral ischemia through Parkin regulation. Environ Toxicol. 2020;35:188–93.
37. Serrano-Pozo A, Frosch MP, Masliah E, Hyman BT. Neuropathological alterations in Alzheimer disease. Cold Spring Harb Perspect Med. 2011;1:a006189.
38. Wang Z, Alzheimer's Disease Neuroimaging I. Brain entropy mapping in healthy aging and Alzheimer's disease. Front Aging Neurosci. 2020;12:596122.
39. Ma RH, Zhang Y, Hong XY, Zhang JF, Wang JZ, Liu GP. Role of microtubule-associated protein tau phosphorylation in Alzheimer's disease. J Huazhong Univ Sci Technol Med Sci. 2017;37:307–12.
40. Szabo L, Eckert A, Grimm A. Insights into disease-associated Tau impact on mitochondria. Int J Mol Sci. 2020;21:6344.
41. Li Y, Xu P, Shan J, Sun W, Ji X, Chi T, et al. Interaction between hyperphosphorylated tau and pyroptosis in forskolin and streptozotocin induced AD models. Biomed Pharmacother. 2020;121:109618.
42. Ren QG, Wang YJ, Gong WG, Zhou QD, Xu L, Zhang ZJ. Escitalopram ameliorates forskolin-induced Tau hyperphosphorylation in HEK239/tau441 cells. J Mol Neurosci. 2015;56:500–8.
43. Wang HH, Li Y, Li A, Yan F, Li ZL, Liu ZY, et al. Forskolin induces hyperphosphorylation of Tau accompanied by cell cycle reactivation in primary hippocampal neurons. Mol Neurobiol. 2018;55:696–706.
44. Zhang Y, Li HL, Wang DL, Liu SJ, Wang JZ. A transitory activation of protein kinase-A induces a sustained tau hyperphosphorylation at multiple sites in N2a cells-imply a new mechanism in Alzheimer pathology. J Neural Transm. 2006;113:1487–97.
45. Caito SW, Aschner M. Mitochondrial redox dysfunction and environmental exposures. Antioxid Redox Signal. 2015;23:578–95.
46. Mastroeni D, Khdour OM, Delvaux E, Nolz J, Olsen G, Berchtold N, et al. Nuclear but not mitochondrial-encoded oxidative phosphorylation genes are altered in aging, mild cognitive impairment, and Alzheimer's disease. Alzheimers Dement. 2017;13:510–9.
47. Manczak M, Park BS, Jung Y, Reddy PH. Differential expression of oxidative phosphorylation genes in patients with Alzheimer's disease. Neuromolecular Med. 2004;5:147–62.
48. Hirai K, Aliev G, Nunomura A, Fujioka H, Russell RL, Atwood CS, et al. Mitochondrial abnormalities in Alzheimer's disease. J Neurosci. 2001;21:3017–23.
49. DuBoff B, Gotz J, Feany MB. Tau promotes neurodegeneration via DRP1 mislocalization in vivo. Neuron. 2012;75:618–32.
50. Sekine S, Kanamaru Y, Koike M, Nishihara A, Okada M, Kinoshita H, et al. Rhomboid protease PARL mediates the mitochondrial membrane potential loss-induced cleavage of PGAM5. J Biol Chem. 2012;287:34635–45.
51. Cummins N, Tweedie A, Zuryn S, Bertran-Gonzalez J, Gotz J. Disease-associated tau impairs mitophagy by inhibiting Parkin translocation to mitochondria. EMBO J. 2019;38:e99360.
52. Tran M, Reddy PH. Defective autophagy and mitophagy in aging and Alzheimer's disease. Front Neurosci. 2020;14:612757.
53. Xu Y, Tang Y, Lu J, Zhang W, Zhu Y, Zhang S, et al. PINK1-mediated mitophagy protects against hepatic ischemia/reperfusion injury by restraining NLRP3 inflammasome activation. Free Radic Biol Med. 2020;160:871–86.
54. Wang Y, Zhu J, Liu Z, Shu S, Fu Y, Liu Y, et al. The PINK1/PARK2/optineurin pathway of mitophagy is activated for protection in septic acute kidney injury. Redox Biol. 2021;38:101767.
55. Butterfield DA, Halliwell B. Oxidative stress, dysfunctional glucose metabolism and Alzheimer disease. Nat Rev Neurosci. 2019;20:148–60.
56. Balaban RS, Nemoto S, Finkel T. Mitochondria, oxidants, and aging. Cell. 2005; 120:483–95.
57. Kang L, Liu S, Li J, Tian Y, Xue Y, Liu X. The mitochondria-targeted anti-oxidant MitoQ protects against intervertebral disc degeneration by ameliorating mitochondrial dysfunction and redox imbalance. Cell Prolif. 2020;53:e12779.
58. Zhu X, Castellani RJ, Moreira PI, Aliev G, Shenk JC, Siedlak SL, et al. Hydroxynonenal-generated crosslinking fluorophore accumulation in Alzheimer disease reveals a dichotomy of protein turnover. Free Radic Biol Med. 2012;52:699–704.
59. Shukla D, Mandal PK, Tripathi M, Vishwakarma G, Mishra R, Sandal K. Quantitation of in vivo brain glutathione conformers in cingulate cortex among age-matched control, MCI, and AD patients using MEGA-PRESS. Hum Brain Mapp. 2020;41:194–217.